This density corresponds to a quasi–Fermi energy of ~2 meV from the bottom of the second miniband. Thus, the width of the electron distribution is much smaller than 2γ at cryogenic temperatures.

With the aid of Eq. 2, Eq. 1 can be rewritten as

$$J_{th} = \frac{\alpha_m + \alpha_w}{g\Gamma} \quad (3)$$

where $\alpha_m = -(\ln R)/L_c = 6.5\ cm^{-1}$ is the mirror loss. We have estimated that the waveguide losses $\alpha_w = 30\ cm^{-1}$ from subthreshold spectra in continuous-wave QC lasers operating at a similar wavelength (*13*). Equation 2 then gives $J_{th} = 3.5\ kA/cm^2$, in reasonable agreement with the experimental value, considering the uncertainty in the value of the waveguide losses.

Our superlattice QC laser—along with intersubband QC lasers (*10*), cascade type-II heterostructure lasers (*15*), and InAsSb/InAlAs strained quantum-well diode lasers (*16*)—are promising mid-IR sources, alternatives to lead-salt diode lasers (*17*). We believe that the key features exploited by the present superlattice scheme—including interminiband transitions of high-oscillator strength, intrinsic population inversion, and high current capability—are particularly favorable for high optical power and long-wavelength operation (8 to 12 μm and beyond).

Note added in proof. We have recently demonstrated laser action at a wavelength of 11 μm.

REFERENCES AND NOTES

1. L. Esaki and R. Tsu, *IBM J. Res. Dev.* **14**, 61 (1970). Miniband formation was directly demonstrated in the optical experiments of R. Dingle, A. C. Gossard, and W. Wiegmann [*Phys. Rev. Lett.* **34**, 1327 (1975)].
2. F. Capasso and A. Y. Cho, *Surf. Sci.* **299–300**, 878 (1994); F. Capasso, J. Faist, C. Sirtori, *J. Math. Phys.* **37**, 14775 (1996).
3. P. Bhattacharya, *Semiconductor Optoelectronic Devices* (Prentice-Hall, Englewood Cliffs, NJ, 1994).
4. C. Waschke *et al.*, *Phys. Rev. Lett.* **70**, 3319 (1993).
5. A Kronig-Penney model with an energy-dependent effective mass m_e^* was used for the calculation of the minibands. The materials parameters are conduction band discontinuity $\Delta E_c = 0.52$eV, m_e^*(GaInAs) = $0.043m_0$, and m_e^*(AlInAs) = $0.078m_0$. Nonparabolicity was treated following C. Sirtori, F. Capasso, J. Faist, S. Scandolo, *Phys. Rev. B* **50**, 8663 (1994). The nonparabolicity coefficient is $\gamma = 1.13 \times 10^{-14}\ cm^2$.
6. M. Helm, *Semicond. Sci. Technol.* **10**, 557 (1995).
7. Electroluminescence data for samples D2135 and D2145 are reported in G. Scamarcio *et al.*, *Appl. Phys. Lett.* **70**, 1796 (1997). These wafers and D2173 have five doped superlattices interleaved with injectors and no waveguide cladding layers to suppress gain-narrowing effects on the spectra. The structures were grown on semi-insulating InP substrates wedged at 45° to collect the luminescence.
8. D. C. Herbert, *Semicond. Sci. Technol.* **3**, 101 (1988).
9. The first and second manifold of eight states of our finite eight-period superlattice were calculated. These define the first and second minibands due to the strong tunnel coupling and the broadening associated with scattering, interface roughness, and doping fluctuations. The interminiband scattering rate $1/\tau_{21}$ is calculated from the lowest state of the second miniband to the highest state of the first miniband, following R. Ferreira and G. Bastard [*Phys. Rev. B* **40**, 1074 (1989)]. The lifetime τ_2 of an electron at the bottom of the second miniband (Eq. 2) is obtained by adding the scattering rates from the bottom of the second miniband to all the states of the first miniband.
10. J. Faist *et al.*, *Science* **264**, 553 (1994). Room-temperature QC lasers are reported in J. Faist *et al.*, *Appl. Phys. Lett.* **68**, 3680 (1996); C. Sirtori *et al.*, *IEEE Photonics Technol. Lett.* **9**, 294 (1997).
11. J. Faist *et al.*, *Phys. Rev. Lett.* **76**, 411 (1996).
12. F. Beltram *et al.*, *ibid.* **64**, 3167 (1990).
13. C. Sirtori *et al.*, *Appl. Phys. Lett.* **66**, 3242 (1995); C. Sirtori *et al.*, *ibid.* **68**, 1746 (1996).
14. J. Faist *et al.*, *ibid.* **65**, 94 (1994).
15. J. I. Malin *et al.*, *ibid.* **68**, 2976 (1996).
16. H. K. Choi, G. W. Turner, H. Q. Le, *ibid.* **66**, 3543 (1995).
17. Z. Shi, M. Tacke, A. Lambrecht, H. Boetner, *ibid.*, p. 2537. For a comprehensive review of lead salt mid-IR lasers, see M. Tacke, *Infrared Phys. Technol.* **36**, 1745 (1996).

18. We are grateful to C. Gmachl for many useful discussions.

11 February 1997; accepted 21 March 1997

Spectroscopic Observation of the Formyl Cation in a Condensed Phase

Peter J. F. de Rege, John A. Gladysz,* István T. Horváth*

The formyl cation, HCO^+, has long been believed to be an important intermediate in the chemistry of carbon monoxide (CO) in acidic environments, but its spectroscopic observation in solution has been elusive. This species was generated by the reaction of CO with the liquid superacid hydrofluoric acid–antimony pentafluoride ($HF\text{-}SbF_5$) under pressure and was observed by nuclear magnetic resonance and infrared spectroscopy. Equilibria between CO in the gas phase, CO dissolved in $HF\text{-}SbF_5$, the SbF_5 adduct of formyl fluoride, and HCO^+ associated with several equilibrating anions of the type $[Sb_xF_{5x+1}]^-$ are proposed to describe the system.

Experimental observation of chemical intermediates plays a crucial role in understanding reaction mechanisms. In addition to verifying the existence of species proposed to explain known reactivity, the discovery of previously unknown intermediates can lead to dramatically different mechanistic explanations for "well-known" reactions. The isolation and identification of positively charged organic species, including carbocations, has provided a solid foundation for current understanding of organic reactions involving electrophilic species (*1*).

Protonation of weakly basic substrates to yield an activated species is central to organic transformations (*2*), enzyme catalysis (*3*), and catalysis of industrial importance (*4*). The strongest known liquid acids, such as $HF\text{-}SbF_5$ and $HSO_3F\text{-}SbF_5$, called superacids because their acidity is higher than that of 100% anhydrous H_2SO_4 (*5*), can protonate extremely weak bases (*6*), even alkanes (*7–9*). Protonation of carbonyl compounds, aromatic systems, alkenes, and many other key classes of organic species has been observed in superacidic environments (*6*, *10*). Although the chemistry of CO in acidic media is well established (*11*), the formyl cation, HCO^+, has not been observed in a condensed phase. The existence of HCO^+ has been surmised on the basis of reactions that indicate electrophilic activation of CO in superacidic media. Gatterman-Koch formylation (*11*, *12*), in which an aromatic compound reacts with CO in an acidic solution to yield an aromatic aldehyde, occurs very readily in the presence of superacids (*13–15*). The formylating agent is believed to be HCO^+ (*6*, *13–15*). The existence of HCO^+ in the gas phase has been well established by microwave, infrared (IR) (*16*), and mass (*17*) spectroscopy, and it is now recognized as one of the most abundant positive ions in deep space (*18*).

The observation of HCO^+ in superacidic solutions has been the goal of many experiments, including (i) direct protonation of CO in a variety of superacidic solutions such as $HSO_3F\text{-}SbF_5\text{-}SO_2ClF$ (*19*), $HSO_3CF_3\text{-}SbF_5\text{-}SO_2ClF$ (*13*), and $HSO_3F\text{-}Au(SO_3F)_3$ (*20*); (ii) abstraction of F^- from H(F)C=O with SbF_5 (*19*); and (iii) dehydration of formic acid (*13*, *19*). In all of these cases, CO was observed in a nonprotonated state, even when the reactions were performed at low temperatures under low CO pressure (<10 atm) to shift the protonation equilibrium (Eq. 1) to the right (*19*)

$$CO + H^+ \leftrightharpoons HCO^+ \quad (1)$$

We expected that, by increasing the partial pressure of CO (P_{CO}) above what had been used for in situ spectroscopic studies,

P. J. F. de Rege and I. T. Horváth, Corporate Research Laboratories, Exxon Research and Engineering Company, Annandale, NJ 08801, USA.
J. A. Gladysz, Department of Chemistry, University of Utah, Salt Lake City, UT 84112, USA.
*To whom correspondence should be addressed.

we could shift the protonation equilibrium to the point where HCO^+ could be observed. High-pressure nuclear magnetic resonance spectroscopy (HP-NMR), in which a single-crystal sapphire tube fitted with a Ti head and valve serves both as reaction vessel and as NMR sample tube, is a powerful tool for in situ examination of chemical reactions occurring under pressures up to 200 atm (*21*). Furthermore, we assumed that, by using the strongest known superacid, HF-SbF_5 (*9*), we could increase the concentration of H^+ and further shift the protonation equilibrium toward HCO^+.

We investigated the reactivity of CO in HF-SbF_5 (1:1) by ^1H, ^{13}C, and ^{19}F HP-NMR, using ^{13}C-labeled CO (Table 1) (*22, 23*). The ^{13}C-NMR (^1H-coupled) at room temperature shows two signals, a doublet of doublets at 179 ppm assigned to the O-complexed SbF_5 adduct of formyl fluoride, H(F)C=O→SbF_5 (*24*) (see below), and a singlet whose chemical shift and intensity relative to that of H(F)C=O→SbF_5 depends on P_{CO}. This latter signal shifts from 145 ppm to 139.5 ppm, and its intensity relative to that of H(F)C=O→SbF_5 increases from 0.43 to 0.75 as P_{CO} is increased from 3 to 85 atm, respectively. This signal (*25*) is assigned to HCO^+ undergoing chemical exchange as depicted in Scheme 1. Variable-temperature HP-NMR (Fig. 1) shows that the species responsible for the two ^{13}C resonances are exchanging slowly on the NMR time scale (equilibrium e in Scheme 1). Depressurization of the sample and repeated freeze-pump-thaw cycles at −78°C lead to complete disappearance of all ^{13}C resonances, indicating that all C-containing species are in equilibrium with CO in the gas phase (equilibria a to d in Scheme 1).

The chemical shift of the HCO^+ resonance, 139.5 ppm, is consistent with the trend observed in a variety of HC(O)X compounds compared with MeC(O)X compounds (Table 2). A ^{13}C chemical shift of 136 ppm, calculated on the basis of ab initio methods (GIAO-MP2) (*26*), is in excellent agreement with our experimental value.

No ^1H-^{13}C coupling is observed in HCO^+, suggesting that the protonation-deprotonation equilibrium (Eq. 1) is rapid on the NMR time scale. This process may involve additional protonation equilibria (Scheme 2). The equilibrium between HCO^+ and COH^+ by means of $HCOH^{2+}$ has been shown by ab initio methods (*27*) to be a viable process in the gas phase and has been proposed to explain the reactivity of CO in superacidic media (*14*). The lack of a separate observable signal in the ^1H-NMR spectrum for HCO^+ is also attributable to rapid protonation-deprotonation equilibria, resulting in a very broad ^1H-NMR resonance. Accordingly, selective decoupling of the acidic ^1H resonance leads to a nuclear Overhauser effect enhancement of the ^{13}C resonance of HCO^+ (*28*). Because the CO-HF-SbF_5 system becomes highly viscous below −40°C, we were not able to use low-temperature NMR to further analyze this rapid exchange process.

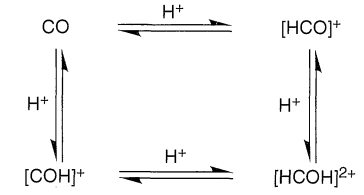

Scheme 2

Our HP-NMR results are supported by IR spectra of the CO-HF-SbF_5 system under CO pressure (Fig. 2) (*29*). Addition of CO (28 atm) to HF-SbF_5 gives a broad band at 2110 cm^{-1} and a sharp band at 1671 cm^{-1}.

Fig. 1 (right). Variable-temperature ^1H, ^{13}C, and ^{19}F HP-NMR spectra of ^{13}CO (5.38 mmol) in HF-SbF_5 (16.4 mmol) in a sapphire NMR tube (total pressure, 26 atm at 25°C). The broad resonance at $\delta(^{19}F) = -113$ (Table 1) is not shown in the ^{19}F spectrum. **Scheme 1 (below).** Proposed equilibria in the superacid HF-SbF_5 under CO pressure.

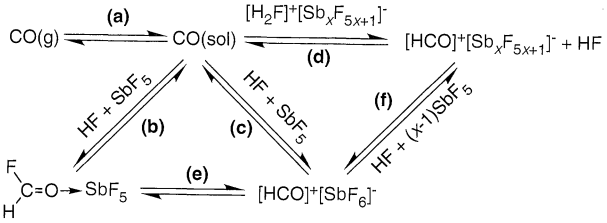

Table 1. HP-NMR data for ^{13}CO-HF-SbF_5 under CO pressure (*22, 23*); ^{13}CO (5.38 mmol); HF-SbF_5 (1:1) (16.4 mmol). Total pressure, 26 atm.

Observed nucleus	Chemical shift (ppm)	Coupling constants (Hz)	Assignment
^1H	7.57	275 (J_{CH}) 98 (J_{HF})	H(F)C=O→SbF_5
^1H	8.14		H_3O^+*
^1H	12.6		HF-SbF_5 and $[HCO]^+[Sb_xF_{5x+1}]^-$†
^{13}C	179	386 (J_{CF}) 275 (J_{CH})	H(F)C=O→SbF_5
^{13}C	139.5		$[HCO]^+[Sb_xF_{5x+1}]^-$†
^{19}F	−205	386 (J_{CF}) 98 (J_{HF})	H(F)C=O→SbF_5
^{19}F	−113		HF-SbF_5 and $[HCO]^+[Sb_xF_{5x+1}]^-$†

*Results from the protonation of trace water, which is present as an impurity (*35*). †Rapidly exchanging on the NMR time scale (see text).

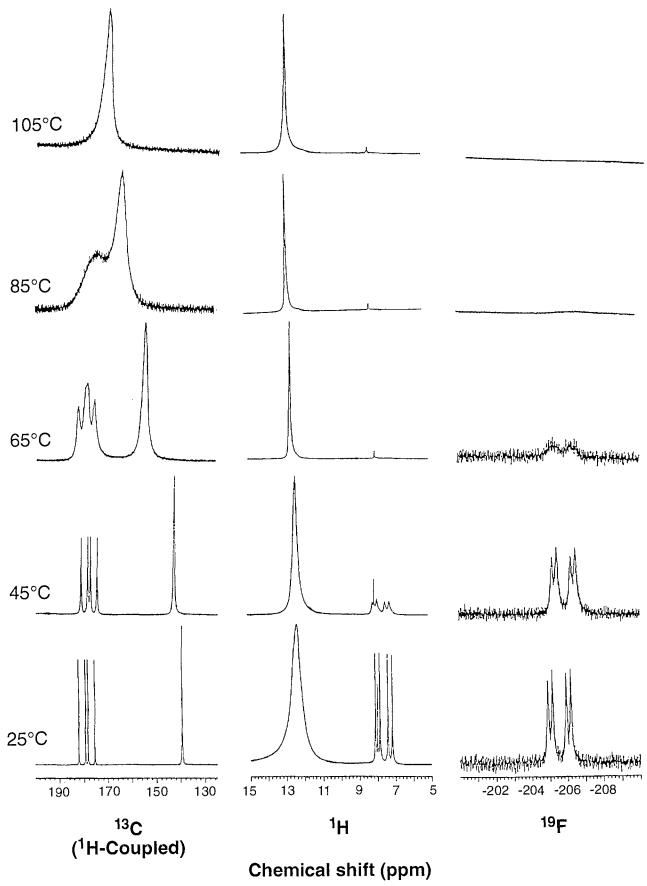

When ^{12}CO was replaced with ^{13}CO (28 atm), the original bands disappeared and new bands at 2060 cm^{-1} and 1629 cm^{-1} appeared, as expected. The band at 1671 cm^{-1} is assigned to ν_{CO} for H(F)C=O→SbF_5, consistent with the large shift from the gas-phase value of free H(F)C=O of 1837 cm^{-1} (*30*). Similar shifts of ν_{CO} are observed for acyl fluorides upon similar complexation (*31*). The band at 2110 cm^{-1} is assigned to HCO^+. The spectrum shows no observable amount of dissolved CO [ν_{CO} for free CO(g) is reported at 2143 cm^{-1} (*20*)], in agreement with the HP-NMR results. Furthermore, the shift in ν_{CO} for HCO^+ in HF-SbF_5 from 2184 cm^{-1}, reported for HCO^+ in the gas phase (*20*), suggests strong interactions with anionic species or SbF_5, or both. The IR data therefore reveal that, although HCO^+ can exist in spectroscopically observable quantities in superacidic liquids, it is by no means best described as "free" HCO^+.

The P_{CO} dependence of the chemical shift and intensity of the HCO^+ ^{13}C resonance relative to that of H(F)C=O→SbF_5 can be explained by Scheme 1. Solutions of SbF_5 in HF are known to involve complex

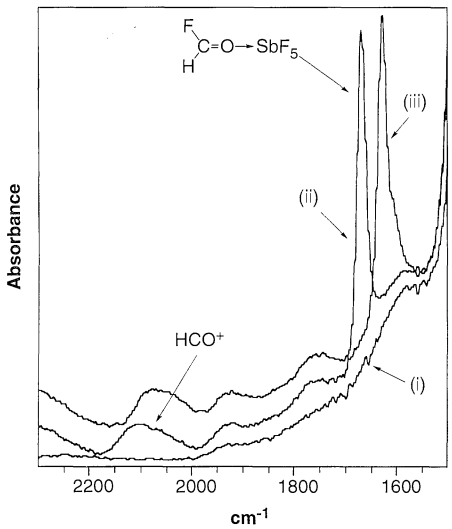

Fig. 2. IR spectra of (i) HF-SbF_5; (ii) HF-SbF_5 + ^{12}CO (28 atm); and (iii) HF-SbF_5 + ^{13}CO (28 atm) (*29*).

Table 2. Carbonyl carbon chemical shift data for formyl and acetyl species (*36*); Me, methyl.

X	δ(^{13}C) (ppm) Me(X) C=O	δ(^{13}C) (ppm) H(X) C=O	Δδ
SbF_6^-	150*	140†	10
OH	176	167	9
OMe	171	161	10
Me	207	200	7
NH_2	178	168	10

*Acylium ion, $[CH_3CO]^+[Sb_xF_{5x+1}]^-$. †Formyl cation, $[HCO]^+[Sb_xF_{5x+1}]^-$, from this work.

equilibria between various anions (Scheme 3) (*9*, *32*). At low ratios of HF to SbF_5, this equilibrium is shifted to the right; at 4:1

$$HF + SbF_5 \rightleftharpoons [H]^+[SbF_6]^- \xrightleftharpoons{[H]^+[SbF_6]^-} [H_2F]^+[Sb_2F_{11}]^- \xrightleftharpoons{(x\text{-}1)\ SbF_5} [H_2F]^+[Sb_xF_{5x+1}]^-$$

Scheme 3

HF-SbF_5, the predominant species is $[H_2F]^+[Sb_2F_{11}]^-$ (*32*). We expect that, in the CO-HF-SbF_5 system at low P_{CO}, the predominant counterion will be $[Sb_xF_{5x+1}]^-$ ($x > 1$). If only H(F)C=O→SbF_5 and $[HCO]^+[SbF_6]^-$ were present in solution, their relative concentrations would be independent of P_{CO}. In contrast, when the ratio of HCO^+ to SbF_5 present in the counterion is not constant, a different P_{CO} dependence is expected for H(F)C=O→SbF_5 and $[HCO]^+[Sb_xF_{5x+1}]^-$ ($x > 1$). As P_{CO} is increased, the products, H(F)C=O→SbF_5 and HCO^+, increasingly dilute the system and this likely shifts equilibrium f in Scheme 1 toward $[HCO]^+[SbF_6]^-$.

In agreement with earlier results (*13*, *19*, *20*), we observed no evidence for HCO^+ or H(F)C=O (free or O-complexed to SbF_5) by HP-NMR or IR when HSO_3F-SbF_5 [a weaker acid by a factor of 1000 than HF-SbF_5 (*9*)] was charged with CO. Furthermore, dilution of HF-SbF_5 with SO_2ClF (1:4) or HF (1:3) resulted in the disappearance of the NMR resonance assigned to HCO^+ even under CO pressure, as previously observed (*13*, *19*, *20*). This result indicates that acid strength plays a crucial role in stabilizing HCO^+ and rendering it spectroscopically observable (by increasing the concentration of H^+ in the protonation equilibrium in Eq. 1). The presence of HCO^+ in weaker superacids is still suggested by the occurrence of Gatterman-Koch formylation in these systems (*13*–*15*), but the equilibrium concentration is obviously much lower. Formyl fluoride itself is an excellent formylating agent in the presence of Lewis acid catalysts (*30*, *33*) and will decompose to HF and CO in the presence of metal catalysts (*34*). These observations are explainable by Scheme 1 as well. The observed formation of H(F)C=O directly from CO in HF-SbF_5 in itself is evidence for involvement of HCO^+, because a likely mechanism would be the protonation of CO followed by electrophilic attack of HCO^+ on $[Sb_xF_{5x+1}]^-$ to form H(F)C=O.

REFERENCES AND NOTES

1. J. March, *Advanced Organic Chemistry* (Wiley-Interscience, New York, 1992).
2. D. Bethell, in *Comprehensive Organic Chemistry*, D. Barton and W. D. Ollis, Eds. (Pergamon, New York, 1979), vol. 1, pp. 411–453; H. Heaney, *ibid.*, pp. 241–360.
3. N. C. Price and L. Steven, *Fundamentals of Enzymology* (Oxford Univ. Press, Oxford, 1982), pp. 157–158; B. C. Gates, *Catalytic Chemistry* (Wiley, New York, 1992), chap. 3; R. K. Thauer, *Angew. Chem. Int. Ed. Engl.* **34**, 2247 (1995).
4. H. Pines, *The Chemistry of Catalytic Hydrocarbon Conversions* (Academic Press, New York, 1981), chap. 1; H. A. Witcoff and B. G. Reuben, *Industrial Chemistry in Perspective*, Part I: *Raw Materials and Manufacture* (Wiley-Interscience, New York, 1980), pp. 226–228.
5. R. J. Gillespie, *Acc. Chem. Res.* **1**, 202 (1968).
6. G. A. Olah, *Angew. Chem. Int. Ed. Engl.* **32**, 767 (1993).
7. ——— and J. Lukas, *J. Am. Chem. Soc.* **90**, 933 (1968); G. A. Olah and R. H. Schlosberg, *ibid.*, p. 2726; G. A. Olah, Y. Halpern, J. Shen, Y. K. Mo, *ibid.* **95**, 4960 (1973).
8. G. A. Olah, *Angew. Chem. Int. Ed. Engl.* **12**, 173 (1973); *Acc. Chem. Res.* **20**, 422 (1987); J. Sommer and J. Bukala, *ibid.* **26**, 370 (1993); P. L. Fabre, J. Devynk, B. Trémillon, *Chem. Rev.* **82**, 591 (1982).
9. T. A. O'Donnel, *Superacids and Acidic Melts as Inorganic Reaction Media* (VCH, New York, 1993).
10. G. A. Olah, G. K. S. Prakash, J. Sommer, *Superacids* (Wiley-Interscience, New York, 1985).
11. G. A. Olah and S. J. Kuhn, in *Friedel-Crafts and Related Reactions*, G. A. Olah, Ed. (Wiley-Interscience, New York, 1964), vol. 3, p. 1153.
12. N. N. Crounse, *Org. React.* **5**, 290 (1949).
13. G. A. Olah, K. Laali, O. Farooq, *J. Org. Chem.* **50**, 1483 (1985).
14. G. A. Olah, F. Pelizza, S. Kobayashi, J. A. Olah, *J. Am. Chem. Soc.* **98**, 296 (1976); O. Farooq, M. Marcelli, G. K. S. Prakash, G. A. Olah, *ibid.* **110**, 864 (1988).
15. M. Tanaka, M. Fujiwara, H. Ando, Y. Souma, *J. Org. Chem.* **58**, 3213 (1993); M. Tanaka, J. Iyoda, Y. Souma, *ibid.* **57**, 2677 (1992); M. Tanaka, M. Fujiwara, H. Ando, *ibid.* **60**, 3846 (1995).
16. R. C. Woods, T. A. Dixon, R. A. Saykally, P. G. Szanto, *Phys. Rev. Lett.* **35**, 1269 (1975); T. Amano, *J. Chem. Phys.* **79**, 3595 (1983).
17. H. Pritchard and A. G. Harrison, *J. Chem. Phys.* **48**, 2827 (1968); A. J. Illies, M. F. Jarrold, M. T. Bowers, *ibid.* **77**, 5847 (1982).
18. D. Buhl and L. E. Snyder, *Nature* **228**, 267 (1970); W. Klemperer, *ibid.* **227**, 1230 (1970).
19. G. A. Olah, K. Dunne, Y. K. Mo, P. Szilagyi, *J. Am. Chem. Soc.* **94**, 4200 (1972).
20. H. Willner and F. Aubke, *Inorg. Chem.* **29**, 2195 (1990); H. Willner *et al.*, *J. Am. Chem. Soc.* **114**, 8972 (1992).
21. I. T. Horváth and J. A. Millar, *Chem. Rev.* **91**, 1339 (1991); I. T. Horváth and E. C. Ponce, *Rev. Sci. Instrum.* **62**, 1104 (1991).
22. NMR experiments were performed with an Oxford Instruments 400-MHz magnet with a Varian Associates Unity 400 System and VNMR Version 5.1 software for data collection and analysis and a Varian Associates 10-mm multinuclear broad-band probe: ^{13}C, 100 MHz; ^1H, 400 MHz; ^{19}F, 375 MHz. Samples were referenced externally with samples of known compounds [C_6F_6; δ(^{19}F) = −162.2 ppm] before insertion of the experimental sample. All spectra were obtained at 25°C unless otherwise indicated.
23. Sapphire HP-NMR tubes were dried at 150°C in an oven. The tubes were charged with HF-SbF_5 (triple-distilled, Aldrich Chemical Company, used as received) within a dry box under Ar (<1 ppm H_2O). ^{13}CO (CIL or Isotec, 99%) and ^{12}CO (MG Industries, research) were added from lecture bottles in quantities determined by a pressure gauge and by difference in weight of the sample tube before and after addition of the gases.
24. Reported values for H(F)C=O couplings compare well with those found in our studies: J_{CH} = 267 Hz; J_{CF} = 369 Hz. The reported J_{HF} = 182 Hz differs significantly from the value that we found, however. We were unable to find a report of the chemical shift of H(F)C=O. G. E. Maciel, J. W. McIver Jr., N. S. Ostlund, J. A. Pople, *J. Am. Chem. Soc.* **92**, 1 (1970); *ibid.*, p. 11; N. Muller and D. T. Carr, *J. Phys. Chem.* **67**, 112 (1963); N. Muller, *J. Chem. Phys.* **36**, 359 (1962).

25. This resonance does not seem to be due to physically dissolved CO, which appears as a singlet near 180 ppm in the strong Lewis acid SbF_5 and in the superacid HSO_3F-SbF_5. The solubility of CO in HSO_3F-SbF_5 is known to be very low (<0.01 M) (*20*) whereas the concentration of the ^{13}C-containing materials in the CO-HF-SbF_5 system is calculated to be at least two orders of magnitude greater.
26. G. A. Olah, personal communication.
27. N. Hartz, G. Rasul, G. Olah, *J. Am. Chem. Soc.* **115**, 1277 (1993). The cation COH^+ has been calculated to be 38 kcal mol^{-1} less stable than HCO^+ in the gas phase (*6*), and it is unlikely that it would be present in observable quantities in these experiments.
28. Selective continuous wave–decoupling (~200 Hz wide) was stepped through the HF-SbF_5 proton resonance (12.5 ppm) in 200-Hz steps, and the intensities of the ^{13}C resonances were monitored.
29. We used two systems to obtain the IR spectra: (i) A ReactIR-1000 System (ASI, Millersville, MD) with a SiComp probe that was mounted to the bottom of a stainless steel pressure cell (volume, 2 ml) fitted with a gas inlet for introduction of CO. (ii) A stainless steel pressure "circle" cell for attenuated total reflectance IR (Spectratech) with a Si rod crystal and fitted with a gas inlet for introduction of CO (cell volume, 2 ml). In both cases, HF-SbF_5 (1 ml) was added to the reactor under anhydrous conditions and the reactor was then charged with ^{13}CO (CIL Isotec, 99%) or ^{12}CO (MG Industries, research grade) from lecture bottles in quantities determined by a pressure gauge. Repeated pressurization-depressurization with ^{13}CO allowed exchange of ^{12}CO with ^{13}CO.
30. G. A. Olah and S. J. Kuhn, *J. Am. Chem. Soc.* **82**, 2380 (1960).
31. _____, W. S. Tolgyesi, E. B. Baker, *ibid.* **84**, 1328 (1962); G. A. Olah *et al.*, *ibid.* **85**, 1328 (1963).
32. R. J. Gillespie and K. C. Moss, *J. Chem. Soc. A* **1966**, 1170 (1966).
33. G. A. Olah, L. Ohannesian, M. Arvanaghi, *Chem. Rev.* **87**, 671 (1987).
34. G. Schatte, H. Willner, D. Hoge, E. Knözinger, O. Schrems, *J. Phys. Chem.* **93**, 6025 (1989).
35. The HF-SbF_5 (1:1) purchased from Aldrich Chemical Company gives a ^1H-NMR resonance for H_3O^+ at 8.86 ppm (verified by addition of H_2O). Upon addition of CO, this peak shifts to 8.14 ppm. These values were referenced against an external $CHCl_3$ standard. The chemical shift of the H_3O^+ ^1H-NMR resonance depends on the acid strength [P. Rimmelin, S. Schwartz, J. Sommer, *Org. Magn. Reson.* **16**, 160 (1981); R. Jost and J. Sommer, *Rev. Chem. Int.* **9**, 171 (1988); D. Zhang, S. J. Rettig, J. Trotter, F. Aubke, *Inorg. Chem.* **35**, 6113 (1996)], which is P_{CO}-dependent (see text).
36. E. Breitmaier and W. Voelter, *Carbon-13 NMR Spectroscopy* (VCH, Weinheim, Germany, 1987).
37. This work was jointly supported by NSF (grant CHE-9401572) and the Exxon Research and Engineering Company. We thank I. Pelczer and G. Kiss for useful discussions, G. A. Olah for providing the results of ab initio calculations of the chemical shift of HCO^+, and K. Smith for use of the ReactIR-1000 system and for help in performing the IR experiments.

23 December 1996; accepted 19 February 1997

Patterned Delivery of Immunoglobulins to Surfaces Using Microfluidic Networks

Emmanuel Delamarche, André Bernard, Heinz Schmid, Bruno Michel, Hans Biebuyck*

Microfluidic networks (μFNs) were used to pattern biomolecules with high resolution on a variety of substrates (gold, glass, or polystyrene). Elastomeric μFNs localized chemical reactions between the biomolecules and the surface, requiring only microliters of reagent to cover square millimeter–sized areas. The networks were designed to ensure stability and filling of the μFN and allowed a homogeneous distribution and robust attachment of material to the substrate along the conduits in the μFN. Immunoglobulins patterned on substrates by means of μFNs remained strictly confined to areas enclosed by the network with submicron resolution and were viable for subsequent use in assays. The approach is simple and general enough to suggest a practical way to incorporate biological material on technological substrates.

The immobilization of ligands on surfaces is a first step in many bioassays, a prerequisite in the design of bioelectronic devices, and a valuable component of certain combinatorial screening strategies. Existing approaches typically expose macroscopic areas of a substrate to milliliter quantities of solution to attach one type of molecule, sometimes using light and specialized chemistries to carry out localized reactions (*1*–*7*). We have explored an alternative approach, namely the use of μFNs to guide nanoliter quantities of reagent to targeted areas on a substrate with submicron control.

We used patterns in an elastomeric support to define a network of conduits for fluids (the μFN) along the surface of a substrate (Fig. 1A) (*8*, *9*). Three walls of these conduits corresponded to molded features in a poly(dimethylsiloxane) (PDMS) rubber (*10*). The fourth wall was the surface of the substrate after it came in contact with the PDMS. Brief exposure of the PDMS to an oxygen plasma before this contact rendered the surface of the conduits hydrophilic and thus allowed a positive capillary action on a liquid introduced at the openings of the conduits (*11*). A tight seal precluding flow between adjacent, noncommunicating capillaries occurred where the PDMS touched the substrate (*12*); spontaneous adhesion between the elastomer and surface maintained this seal without requiring additional pressure. We applied the elastomer to Au, glass, and Si-SiO_2 surfaces previously activated by formation of a hydroxylsuccinimidyl ester to achieve chemical coupling with pendant amino groups common to proteins. These substrates had enough reactivity so that monolayer quantities of immunoglobulin G (IgG) were readily fixed to the surface, preventing their detachment in the ensuing washing steps (*13*). We followed the attachment of IgGs on the surface by ellipsometry (*14*) and waveguide techniques (*15*) over the large areas (~1 mm^2) probed by these methods to confirm the extent of reaction and the quality of attachment.

We designed the network as a system of two pads, each with lateral dimensions of 3 mm by 1 mm, connected by 100 channels, each 3 mm long, 3 μm wide, and separated by 0.8 μm (Fig. 1B). The channels were 1.5 μm deep, which provided an aspect ratio that allowed the formation of well-defined and stable capillaries in the PDMS. Deeper capillaries proved prone to collapse, either spontaneously (because of gravity) or during one of the processing steps; substantially shallower capillaries tended to block, provide poor mass transport of proteins, or deform onto the surface (*16*). With a μFN of the above dimensions, delivery of proteins onto the substrate could be homogeneous over distances of a few millimeters while still providing practical quantities of covalently attached material for convenient screening using enzyme-linked immunosorbent assay (ELISA) methods or ordinary fluorescence microscopy. The independence of capillaries in a network also allows simultaneous attachment of different biomolecules in each zone of flow (Fig. 1C). The topology of the network ensures a minimal use of solutions needed to derivatize the surface and can concentrate zones of flow into small fields of view without compromising their integrity.

Depletion of proteins from a dilute solution confined in small volumes can result from the loss of material onto the walls of the conduits or its incorporation into the bulk part of the PDMS (*17*). Flow through the capillaries into a second, hydrophilic pad avoided such loss of material available for the coupling step, where diffusion of the dilute protein from the filling pad might be insufficient. Depletion could also be cir-

E. Delamarche, H. Schmid, B. Michel, H. Biebuyck, IBM Research Division, Zurich Research Laboratory, CH-8803 Rüschlikon, Switzerland.
A. Bernard, IBM Research Division, Zurich Research Laboratory, CH-8803 Rüschlikon, Switzerland, and Biochemisches Institut der Universität Zürich, Winterthurerstrasse 190, CH-8057 Zürich, Switzerland.

*To whom correspondence should be addressed. E-mail: hbi@zurich.ibm.com